Hydraulic Conductivity Modeling of Fractured Rock at Grasberg Surface Mine, Papua-Indonesia

Tedy Agung Cahyadi[1,*], Lilik Eko Widodo[2], Zuher Syihab[2], Sudarto Notosiswoyo[2] & Eman Widijanto[3]

[1]Mining Engineering Graduate Program,
Faculty of Mining and Petroleum Engineering, Bandung Institute of Technology
Jalan Ganesha 10, Bandung, 40132, Indonesia
[2]Research Group of Earth Resource Exploration,
Faculty of Mining and Petroleum Engineering, Bandung Institute of Technology,
Jalan Ganesha 10, Bandung, 40132, Indonesia
[3]Surface Mine GeoEngineering, PTFI, Grasberg Surface Mine, Papua, 99930, Indonesia
*E-mail: tedyagungc.students.itb@gmail.com

Abstract. Packer tests and slug tests were conducted at 49 points at the Grasberg surface mine, Indonesia to obtain hydraulic conductivity data. The HC-system approach, which relies on rock quality designation, lithology permeability index, depth index, and gouge content designation, was applied. Geotechnical drill holes in 441 locations, consisting of 4,850 points of information, were used to determine the K values using the equation $K = 2x10^{-6}x\ HC^{0.5571}$. The K values, which were within the range of 10^{-8} and 10^{-5} m/s, were distributed into five alternative 3D distributions using Ordinary Kriging (OK) and Artificial Neural Network (ANN). The result of the ANN modeling showed that some of the K values, with log K varying from -10.51 m/s to -3.09 m/s, were outside the range of the observed K values. The OK modeling results of K values, with log K varying from -8.12 m/s to -5.75 m/s, were within the range of the observed K values. The ANN modeled K values were slightly more varied than the OK modeled values. The result of an alternative OK modeling was chosen to represent the existing data population of flow media because it fits well to the geological conditions.

Keywords: *artificial neural network (ANN); fractured rock; HC-system; spatial hydraulic conductivity; ordinary kriging (OK).*

1 Introduction

The hydrogeological conditions of hard rock (metamorphic and igneous) in mine sites are commonly characterized by a fractured condition under complex geological settings consisting of a fault zone and fracture networks [1]. The Grasberg Mine, PT Freeport Indonesia, Papua is situated in fractured-groundwater-flow media. The hydraulic properties, among which hydraulic conductivity (K), are related to the following parameters: in-situ stress, rock matrix properties, fracturing including aperture, density, persistence,

Received March 21st, 2016, 1st Revision June, 1st, 2016, 2nd Revision July 4th, 2016, 3rd Revision September 14th, 2016, 4th Revision January 23rd, 2017, Accepted for publication February 13th, 2017.
 ISSN: 2337-5779, DOI: 10.5614/j.eng.technol.sci.2017.49.1.3

orientation, interconnectivity, filling material and roughness [2]. Other researchers have discussed hydraulic conductivity estimation, usually based on empirical equations, which shows a decrease of hydraulic conductivity with depth [3,4].

It is known that the stability of the slope in the Grasberg Mine is prone to groundwater influence. Thus, it is important to build a robust groundwater model to study several aspects of the area, including the dewatering process. Groundwater modeling requires 3D distributed data of hydraulic conductivity (K) to be able to place dewatering drilling targets accurately. Optimization of dewatering drilling targets can be achieved by utilizing reliable hydraulic parameters for the groundwater model. The parameters can be obtained through field measurements, such as packer tests and slug tests. These tests are considered very costly during the early stages of mine-site characterization [5]. In order to reduce the costs, a new method predicting hydraulic conductivity distribution was successfully applied by comparing in-situ packer test data with geotechnical drill log data, such as rock quality designation (RQD), lithology permeability index (LPI), depth index (DI) and gouge content index (GCI). This method was developed by Hsu, *et al.* [6] and is called HC-system.

In order to acquire the spatial distribution for the entire domain within the field, a geostatistical method was applied. This method considers subsurface formations as mathematical models of random fields in which the spatial correlations of the parameters are statistically inferred from observations [7]. Ordinary Kriging (OK) is one of the most common spatial estimators for a single variable. OK calculates a value at unsampled points using a weighted summation of n samples. Cahyadi, *et al.* [8] have successfully modeled a 3D distribution of hydraulic conductivity based on 34 data from constant head permeability slug tests. Apart from the geostatistical method, an artificial neural network (ANN) method was also applied to estimate the hydraulic conductivity at unsampled points.

ANN is a computational system that mimics biological neural processing to determine the specific relationship between input and output variables. This process can be achieved and validated by training based on a number of input and output pairs [9]. Modeling of the spatial distribution of hydraulic conductivity with ANN can be conducted by using a segmentation method [10].

The purposes of this study were: (1) to estimate the K values at points for which a geotechnical log data are available but no hydraulic test data; (2) to choose the best 3D distribution alternative of the hydraulic conductivity model under limited in-situ data using HC-system, which was approached using two different methods, i.e. ANN and OK; (3) to compare the alternative hydraulic

conductivity models constrained by the geological conditions at the Grasberg Mine.

2 Geological Settings

Following McDonald, *et al*. [11] and McDowell [12], the geological settings of the study area can be summarized as follows. The Grasberg open-pit mine is located in the Papuan Fold and Thrust Belt, more particularly in the south of the Mobile Belt. Late Miocene to Pliocene calc-alkaline magmatism pierces the fold and thrust belt and the related porphyry copper deposit, i.e. Grasberg in West Papua. The structures in the location are as follows: the Yellow Valley Syncline, first fault set including Idenberg #1 Fault, Meren Valley #2 Fault, Fairy Lakes Fault, second fault set including Barat Laut Fault, Idenberg #2 Fault, and third fault set including Grasberg Fault, Carstensz Valley Fault, and New Zealand Pass Fault (Figure 1). There are two fundamentally different protoliths within the Grasberg Intrusive Complex (GIC): a Dalam Volcanic Breccia Group (DBG) and a Quartz Monzodiorite Group (QMG). The DBG includes the Dalam Andesite and the Dalam Fragmental units. The QMG includes the Early Kali, Late Kali, Main Grasberg Intrusive, and the Dalam Diorite units. The hydrothermal alteration types are roughly concentrically zoned within the diatreme. Alteration types commonly overlap and create several types of materials, including Poker Chip, Dalam Fine, and Hard Zone.

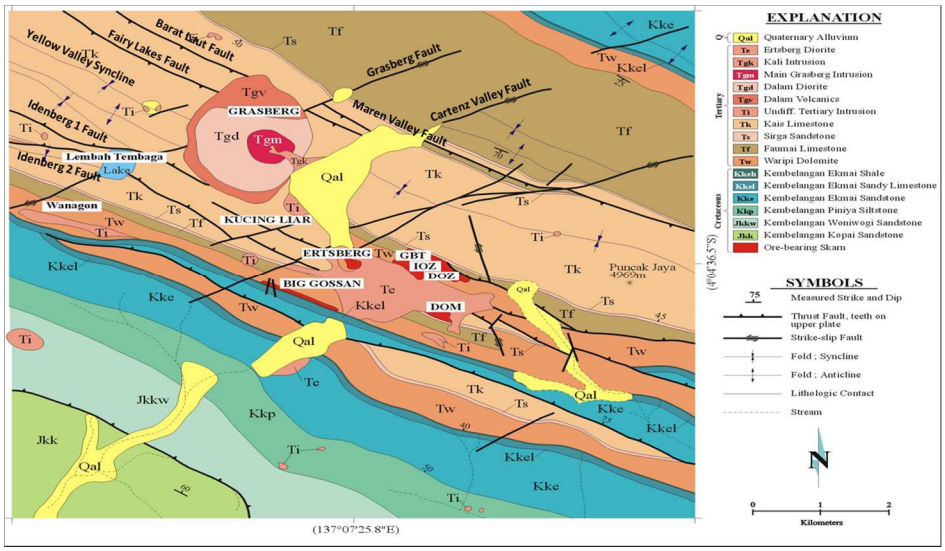

Figure 1 Geological map of Grasberg (modified from Suwardi, *et al*. [13]).

The stratigraphy of the Grasberg mine, according to Suwardi, *et al*. [13] and Hill, *et al*. [14], can be described as follows: alluvium (Quaternary alluvial, colluvium, and glacial); intrusions (Dalam Intrusion, Main Grasberg Intrusion, and Kali Intrusion); the Kais Formation (limestone with low fracture and high fracture, and coarse fragmentation); the Sirga Formation (sandstone with medium to coarse fragmentation); the Faumai Formation (massive limestone); the Waripi Formation (dolomite); the Ekmai Formation (sandstone); the Piniya Formation (mudstone); the Woniwogi Formation (sandstone); and the Kopai Formation (sandstone).

3 Hydrogeological Settings

Grasberg is one of the largest open-pit mines in the world, with a 3.5 km diameter and a depth of 1.1 km. Rainfall is high in the area, more than 4,000 mm/year, with 1,470 ha of catchment area. The rainfall impacts the quantity of precipitation of 25,500 gpm, from which 55% runs off [15]. Based on field observation, the groundwater system at the Grasberg Mine can be divided into two different types. The first is a primary aquifer, which is controlled by porosity, consisting of overburden material, alluvial material, and the Sirga Formation. The other one is a secondary aquifer, controlled by fracture inter-connection and consisting of the Kais Formation, which is dominated by limestone. According to Silaen, *et al*. [16], the occurrence of aquifers in and around the GIC is related to secondary geological structures. Based on the existing geological information from investigation drilling, the conceptual hydrogeology of the Grasberg mine can be described as follows [16]:

1. GIC (locally permeable where structures occur), comprising three intrusions (Dalam Intrusion Complex, Kali Intrusion Complex, and Main Grasberg Intrusive Complex (MGI));
2. inner contact zone (permeable) between the GIC and the Heavy Sulphide Zone (HSZ);
3. HSZ (variable permeability);
4. outer contact zone (permeable) between the HSZ and adjacent marble zone;
5. marble zone (low permeability);
6. limestone country rocks outside the GIC (permeable, where secondary structures occur).

The Dalam fine material has the lowest hydraulic conductivity compared to the other materials. HSZ has higher hydraulic conductivity than the Dalam fine material, which is suspected to provide a conduit for the surface water forming a perched groundwater system [16].

4 Methods

The field study was completed on March 2015. Data collection consisted of hydraulic conductivity tests by packer test, slug test and geotechnical log data from drill holes. Hsu, *et al*. [6] and Iskandar, *et al*. [17] used packer tests to develop empirical models of hydraulic conductivity. Following the previous researches, this study was aimed at developing the following five alternative empirical models:

1. Empirical model – Alternative I: based on 18 data from packer tests, of which 14 data were used for estimation and 4 data for validation.
2. Empirical model – Alternative II: based on 31 data from slug tests, of which 26 data were used for estimation and 5 data for validation.
3. Empirical model – Alternative III: based on a combination of packer test and the slug test data, 49 in total, of which 40 data were used for estimation and 9 data for validation.
4. Empirical model – Alternative IV: based on all packer test data, which were used for estimation while the slug test data were used for validation.
5. Empirical model – Alternative V: based on all slug test data, which were used for estimation while the packer test data were used for validation.

The packer test data were available from 2 boreholes and 18 target points. Additionally, slug test data were available from 31 boreholes. Five alternative empirical models were built to estimate hydraulic conductivity using 441 drill hole data, or 4,850 additional isotropic hydraulic conductivity points (Figure 2). Then, the observed data and HC extracted from the models were spatially distributed using ANN and OK.

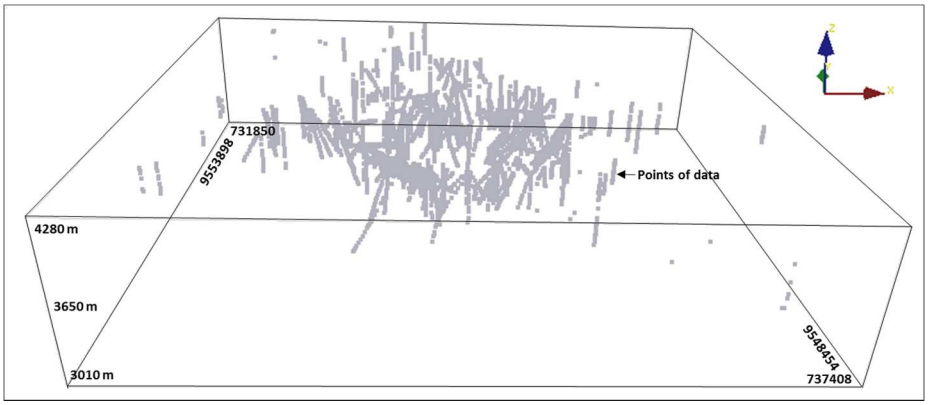

Figure 2 3D spatial distribution of data points.

ANN was chosen because of its capability to describe non-linear relationships between parameters – e.g. the distribution of hydraulic conductivity against position. For the purpose of comparison, 3D distribution of hydraulic conductivity was performed with OK. Figure 3 shows the steps carried out in this study. It was initiated by empirical modeling of hydraulic conductivity according to the HC-system. The results were then 3-dimensionally distributed using the OK method [8] and soft computing using ANN [10]. The best performing model was verified using a statistical approach and geological model correlation.

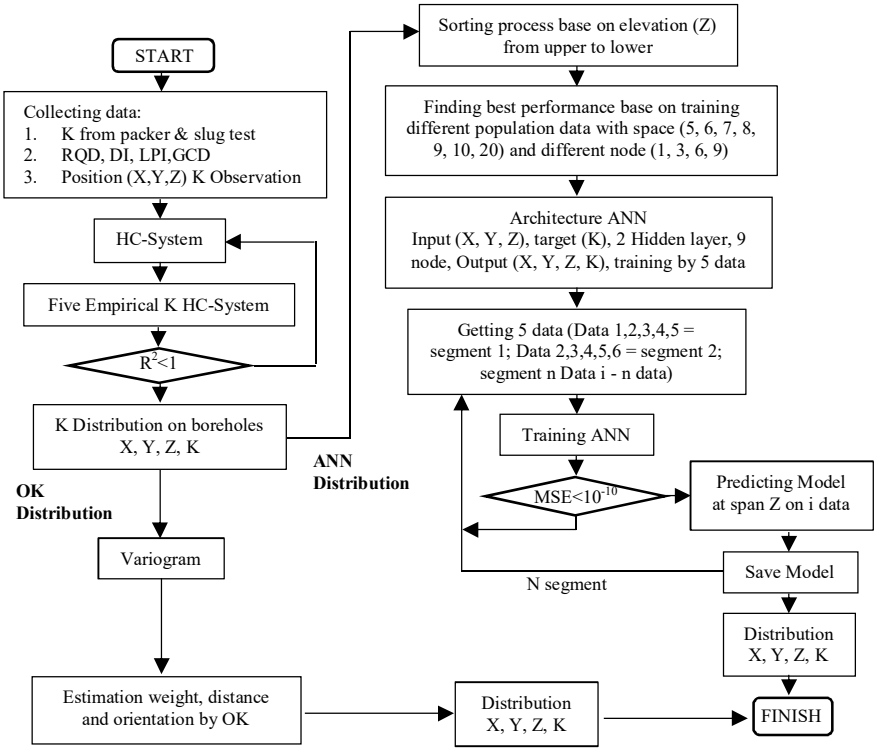

Figure 3 Schematic diagram of 3D hydraulic conductivity distribution modeling.

5 Result

5.1 HC-System

Five alternative models were built using packer test data and slug test data and their combination to obtain isotropic hydraulic conductivity based on

information from RQD, LPI, DI, GCD from 441 geotechnical drill holes, or 4,850 points.

1. *Rock Quality Designation (RQD)*

$$RQD = \frac{\sum R_S}{R_T} \times 100\% \quad (1)$$

Following Deere, *et al*. [18], the RQD value was defined as the cumulative length of core pieces longer than 100 mm in a run (R_S) divided by the total length of the core run (R_T).

2. *Lithology Permeability Index (LPI)*

Different lithologies affect permeability variation in the field, according to the following assumption: the bigger the grain size, the higher the permeability of a lithology. The LPI index for the Grasberg Mine was developed according to Singhal and Gupta [19], Spitz and Moreno [20], Bear [21], Hsu, *et al*. [6]. The rating of LPI values for the Grasberg Mine is listed in Table 1.

Table 1 Rating of LPI values based on lithology in the study area.

Lithology	Suggested rating	Lithology	Suggested rating
Andesite	0.15	Sandy dolomite	0.95
Trachyandesite	0.15	Silty dolomite	0.95
Hydrothermal breccia	0.1	Gravel	1
Intrusive breccia	0.1	Limestone	0.7
Diorite	0.15	Limestone breccia	1
Porphyritic diorite	0.15	Dolomitic limestone	0.7
Monzonite	0.15	Sandy limestone	0.4
Porphyritic monzonite	0.1	Silty limestone	0.3
Quartz diorite	0.15	Mudstone	0.3
Quartz diorite porphyritic	0.15	Shale	0.5
Quartz monzonite	0.15	Shale carbonaceous	0.75
Quartz monzonite porphyritic	0.15	Shale limey	0.6
Tuff	1	Sandstone	1
Alluvium	1	Limestone sandstone	0.95
Colluvium	1	Sandstone breccia	1
Rehandle Material	1	Sandstone breccia	1
Sedimentary breccia	1	Limey sandstone	0.3
Tectonic breccia	1	Silty sandstone	0.3
Conglomerate	1	Siltstone	0.3
Clay	0.3	Dolomitic siltstone	0.2
Dolomite	0.7	Limey siltstone	0.3
Dolomite breccia	0.85	Sandy siltstone	0.2
Limey dolomite	0.7		

3. *Depth Index (DI)*

$$DI = 1 - \frac{L_c}{L_T} \tag{2}$$

Following Hsu, *et al*. [6], L_T is the total length of the borehole; L_c is the depth located at the middle of the observation test interval in the borehole. Since Hsu, *et al.* [6] used only vertical boreholes, vertical transformation was performed for inclined boreholes in this study. This method was also applied by Iskandar, *et al.* [17].

4. *Gouge Content Designation (GCD)*

The value of GCD was assumed to be proportional to RQD: as RQD increases, permeability decreases. The GCD value was estimated to range between 0.9 and 1.0. Gouge content thickness was not recorded in the regular drill core logs. The HC index is an empirical method to estimate the HC-value (HC), and in this study it was then plotted against the hydraulic conductivity from the observation test in the same zone. Following Hsu, *et al*. [6], the HC index is described by Eq. (3).

$$HC = \left(1 - \frac{RQD}{100}\right).(DI).(1 - GCD).(LPI) \tag{3}$$

where:
HC : HC value
RQD : rock quality designation
DI : depth index
GCD : gouge content designation
LPI : lithology permeability index

Based on the field test results using packer tests and slug tests (Table 2), the hydraulic conductivity values in this study were heterogeneous. Structure and fracture are controlled by tectonic setting and geological process. The location at which the hydraulic packer tests and slug tests was performed is dominated by igneous and sedimentary rock. The K value varies even within similar lithologies, e.g. in limestone the value ranges from 7.53 x 10^{-9} to 1.09 x 10^{-6} m/s.

A regression analysis was applied to estimate the dependence of the HC index on the hydraulic conductivity from 49 pairs of packer test data and slug test data from the same zone. The RQD of each test interval was calculated using Eq. (1). The LPI of each test interval was determined by conversion using Table 1 and the value of DI of each test interval was calculated using Eq. (2). The GCD was assumed, due to the limited core drilling data. Hence, an empirical model of the hydraulic conductivity could be obtained, which follows the power law

relationship. Finally, five empirical HC models were developed, as depicted in Figure 4.

Different empirical models may give unique responses to each hydraulic conductivity estimation. Hsu, *et al.* [6] and Iskandar, *et al.* [17] relied on packer test data to get an empirical model of hydraulic conductivity. In this study, the authors tried to apply all useable resources to develop the empirical model. A number of slug tests was targeted to specific lithology to predict its hydraulic conductivity. Different empirical models (see Figure 4) were used to predict hydraulic conductivity in drill holes without observation data. A sensitivity analysis for the empirical models was carried out by comparing the empirical models' values with real values of hydraulic conductivity in the field. The five empirical HC models are expressed in Eqs. (4) to (8), respectively.

$$K = 7 \times 10^{-6} \times (HC)^{0.8125}, R^2 = 0.825 \quad (4)$$

$$K = 2 \times 10^{-6} \times (HC)^{0.5866}, R^2 = 0.794 \quad (5)$$

$$K = 2 \times 10^{-6} \times (HC)^{0.5571}, R^2 = 0.716 \quad (6)$$

$$K = 7 \times 10^{-6} \times (HC)^{0.8132}, R^2 = 0.861 \quad (7)$$

$$K = 2 \times 10^{-6} \times (HC)^{0.6034}, R^2 = 0.761 \quad (8)$$

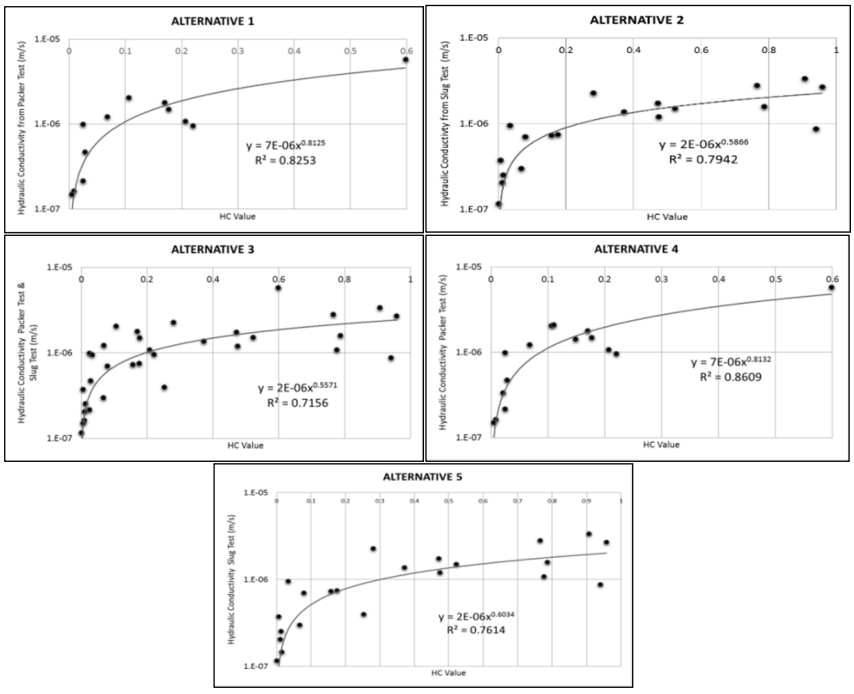

Figure 4 Relationship between observed hydraulic conductivity and HC values.

Table 2 Result of calculation of HC values in each packer and slug test zone.

Hole ID	Lithology	K packer & slug test (m/s)	1-(RQD/100)	DI	1-GCD	LPI	HC
VZW-094	Hornblende	5.79×10^{-6}	0.9	0.92	0.9	0.8	0.598
VZW-094	Volcanic Breccia	4.73×10^{-7}	0.6	0.76	0.6	0.1	0.028
VZW-094	Volcanic Breccia	2.16×10^{-7}	0.6	0.68	0.6	0.1	0.025
VZW-094	Volcanic Breccia	7.78×10^{-8}	0.4	0.59	0.4	0.1	0.009
VZW-094	Volcanic Breccia	1.63×10^{-7}	0.4	0.52	0.4	0.1	0.008
VZW-094	Volcanic Breccia	4.54×10^{-8}	0.2	0.43	0.2	0.1	0.002
VZW-094	Scarn	1.50×10^{-6}	0.8	0.34	0.8	0.8	0.177
VZW-094	Limestone	4.27×10^{-8}	0.2	0.26	0.2	0.5	0.005
VZW-094	Limestone	3.37×10^{-7}	0.5	0.16	0.5	0.5	0.021
VZW-094	Limestone	1.51×10^{-7}	0.4	0.05	0.4	0.5	0.004
GHD-3885-26	Volcanic Breccia	1.08×10^{-6}	0.9	0.85	0.9	0.3	0.207
GHD-3885-26	Volcanic Breccia	1.43×10^{-6}	0.9	0.61	0.9	0.3	0.149
GHD-3885-26	Volcanic Breccia	2.06×10^{-6}	0.9	0.43	0.9	0.3	0.105
GHD-3885-26	Hornblende	9.64×10^{-7}	0.9	0.33	0.9	0.8	0.220
GHD-3885-26	Hornblende	1.79×10^{-6}	0.9	0.26	0.9	0.8	0.169
GHD-3885-26	Hornblende	2.11×10^{-6}	0.9	0.17	0.9	0.8	0.110
GHD-3885-26	Hornblende	1.23×10^{-6}	0.9	0.10	0.9	0.8	0.067
GHD-3885-26	Hornblende	9.97×10^{-7}	0.9	0.03	0.9	0.8	0.024
CSTG-01	Alluvium	3.98×10^{-7}	0.6	0.87	0.6	0.8	0.252
CSTG-02B	Alluvium	1.75×10^{-6}	0.9	0.72	0.9	0.8	0.470
VZW-17S	Alluvium	1.52×10^{-6}	0.9	0.80	0.9	0.8	0.521
OHS-21	Overburden	8.79×10^{-7}	1	0.93	1	1	0.940
VZW-25A	Overburden	2.71×10^{-6}	1	0.95	1	1	0.958
VZW-31	Quartz	9.57×10^{-7}	0.5	0.65	0.5	0.2	0.033
VZW-58	Quartz	1.38×10^{-6}	1	0.52	1	0.7	0.371
VZW-74	Quartz	3.97×10^{-8}	0.2	0.94	0.2	0.2	0.008
VZW-50	Quartz	3.76×10^{-7}	0.4	0.30	0.4	0.1	0.005
VZW-55	Quartz	2.55×10^{-7}	0.4	0.78	0.4	0.1	0.013
VZW-62	Quartz	1.74×10^{-8}	0.5	0.56	0.5	0.1	0.014
VZW-17	Granodiorite	1.17×10^{-7}	0.1	0.35	0.1	0.1	0.0003
VZW-76	Trachyandesite	4.13×10^{-8}	0.1	0.68	0.1	0.1	0.0007
VZW-51	Volcanic Breccia	7.36×10^{-7}	0.8	0.81	0.8	0.3	0.157
VZW-29	Limestone	7.53×10^{-9}	0.1	0.25	0.1	0.1	0.0003
VZW-29S	Limestone	5.46×10^{-8}	0.2	0.76	0.2	0.1	0.003
VZW-40	Limestone	1.59×10^{-6}	0.9	0.97	0.9	1	0.786
VZW-49D	Limestone	7.52×10^{-7}	0.6	0.97	0.6	0.5	0.175
VZW-52	Limestone	1.09×10^{-6}	0.9	0.95	0.9	1	0.775
VZW-53A	Limestone	2.82×10^{-6}	0.9	0.94	0.9	1	0.765
VZW-59	Limestone	7.05×10^{-7}	0.6	0.43	0.6	0.5	0.078
VZW-63	Limestone	3.38×10^{-6}	1	0.90	1	1	0.906
VZW-68	Limestone	2.27×10^{-6}	1	0.27	1	1	0.280
VZW-69	Limestone	1.21×10^{-6}	1	0.47	1	1	0.474
VZW-71	Sandstone	2.06×10^{-7}	0.3	0.12	0.3	0.9	0.010
VZW-75	Limestone	3.01×10^{-7}	0.5	0.52	0.5	0.5	0.066
VZW-39	Limestone	2.04×10^{-8}	0.2	0.49	0.2	0.1	0.002
VZW-61	Limestone	7.36×10^{-8}	0.2	0.76	0.2	0.1	0.003
VZW-73	Limestone	5.29×10^{-8}	0.2	0.84	0.2	0.1	0.003
VZW-245	Volcanic Breccia	1.14×10^{-8}	0.5	0.20	0.5	0.1	0.005
VZW-244	Limestone	1.46×10^{-7}	0.5	0.55	0.5	0.1	0.014

The correlation between the values from observation and each empirical HC model was then verified. Initially, 4 target points were used to verify the model, i.e. the following drill holes: VZW-094 from 158 m to 183 m; VZW-094 from 233 m to 267 m; GHD-3885-26 from 50.19 m to 68.96 m; and GHD-3885-26 from 121.84 m to 132.57 m. Secondly, 5 points target points were used to verify the model, i.e. the following drill holes: CSTG-01, VZW-74, VZW-52, VZW-245, and VZW-244. Thirdly, the first and second targets were combined. Fourthly, verification of the empirical HC model was carried out by using all slug test data. Lastly, verification was carried out based on the packer test data from VZW094 and GHD-3885-26 (Table 2). The correlation parameters for every alternative model are shown in Figure 5. The verification was then used to determine the rock mass hydraulic conductivity for other drill holes surrounding the Grasberg Mine.

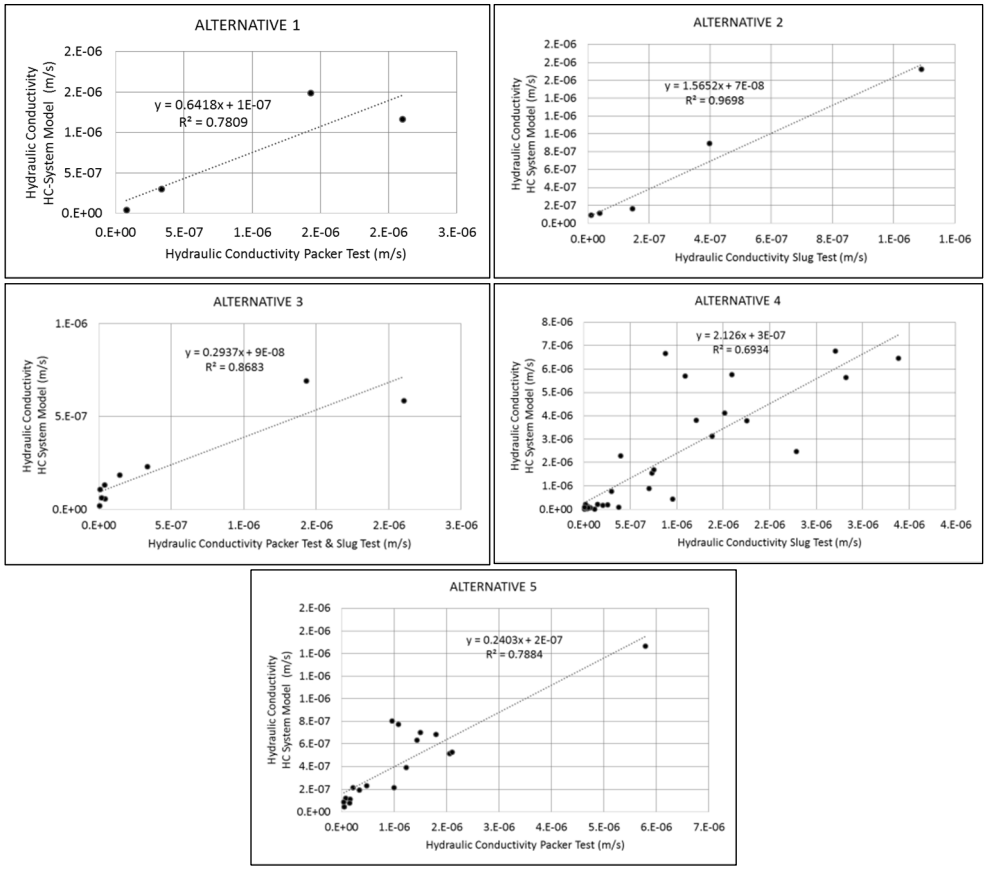

Figure 5 Correlation between modeled K according HC-system and observed K.

5.2 Ordinary Kriging (OK)

Before utilizing the OK method for hydraulic conductivity prediction at unsampled points, a semivariogram was required for each alternative to determine the spatial correlation and data distribution pattern. The semivariograms were used in different directions (0°, 45°, 90°, 135°) and omnidirectional.

The five alternatives are shown with different nugget and sill values (Figure 6). The smallest nugget value was found in the third alternative (c). The semivariograms show distances of influence of 2,100 m and 1,250 m in the horizontal and the vertical direction, respectively. A summary of the semivariograms is shown in Table 3. Estimation according to OK was carried out using the Stanford Geostatistical Modeling software [22]. Because the hydraulic conductivity values were very small, their logarithms were taken to simplify the analysis. The values of hydraulic conductivity were transformed to a logarithmic scale and then normalized after analysis.

Table 3 Summary of semivariograms.

Model	Azimuth: 0°, 45°, 90°, 135°			Azimuth: omnidirectional		
	Nugget	Sill	Range (m)	Nugget	Sill	Range (m)
Alternative 1	0.09	0.27	1,250	0.09	0.24	2,100
Alternative 2	0.045	0.14	1,250	0.045	0.13	2,100
Alternative 3	0.04	0.13	1,250	0.04	0.11	2,100
Alternative 4	0.07	0.28	1,250	0.07	0.24	2,100
Alternative 5	0.045	0.15	1,250	0.045	0.13	2,100

To measure the quality of the 3D hydraulic conductivity model, a verification process was conducted. The authors used some observations to verify the implementation in the field. The hydraulic conductivity model according to HC-system was then distributed 3-dimensionally by means of a block model with a grid size of 50 m x 50 m x 15 m. From 441 geotechnical drill holes, 4,850 hydraulic conductivity points were retrieved from HC-system. The points were then distributed to model the spatial distribution of hydraulic conductivity in the study area with total dimensions of about 5 km x 5 km x 1.2 km.

Figure 7 shows the different quality levels of the validation models. The third alternative had a significant coefficient of determination of 0.63. The relatively higher coefficient of determination compared to the other alternatives is in agreement with the smaller nuggets obtained from the semivariogram. The OK method was alternatively used for estimation of unsampled points. For comparison, ANN was also used to predict hydraulic conductivity at the unsampled points.

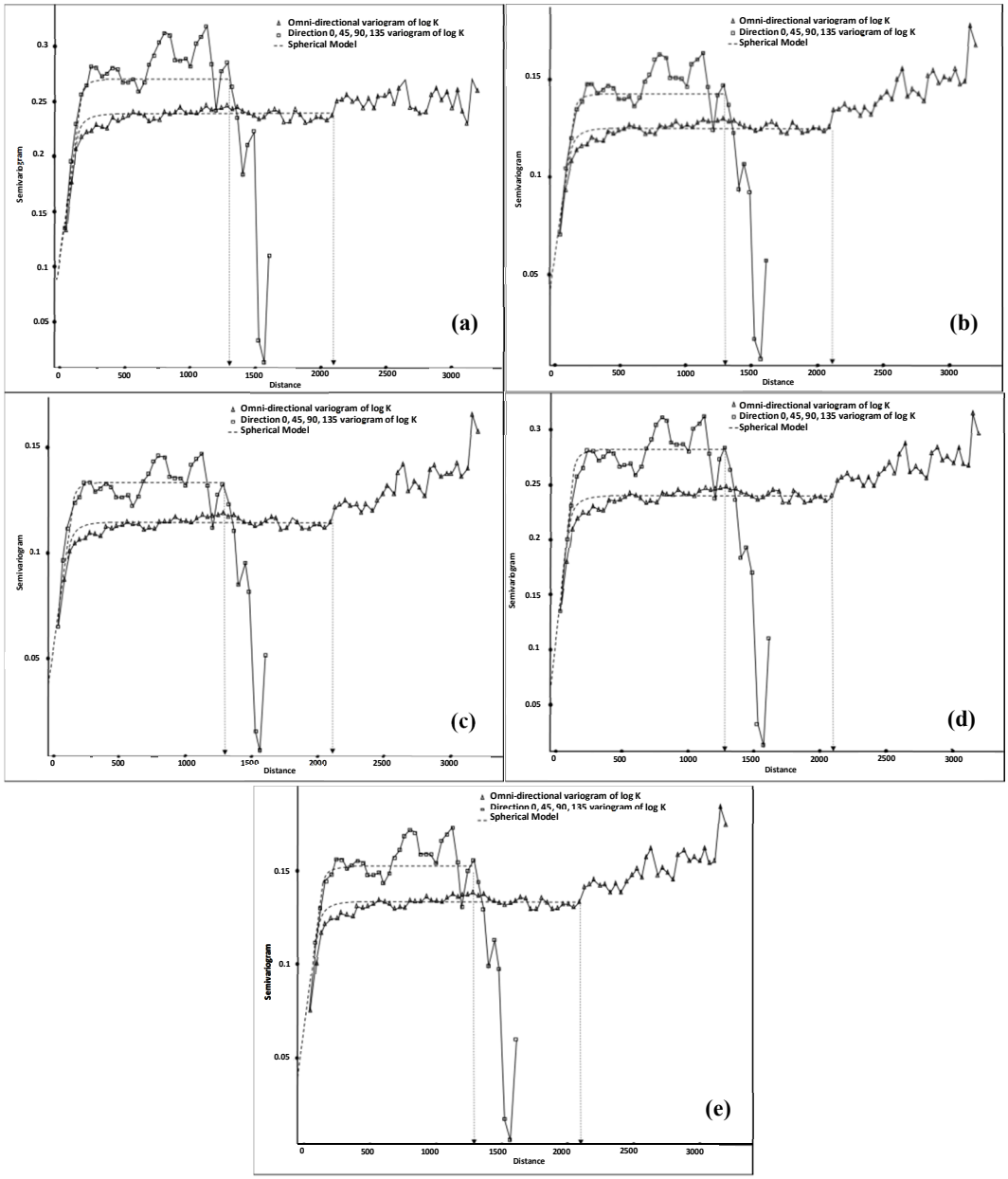

Figure 6 Semivariogram distribution from observed and modeled HC-system: (a) first alternative; (b) second alternative; (c) third alternative; (d) fourth alternative; and (e) fifth alternative.

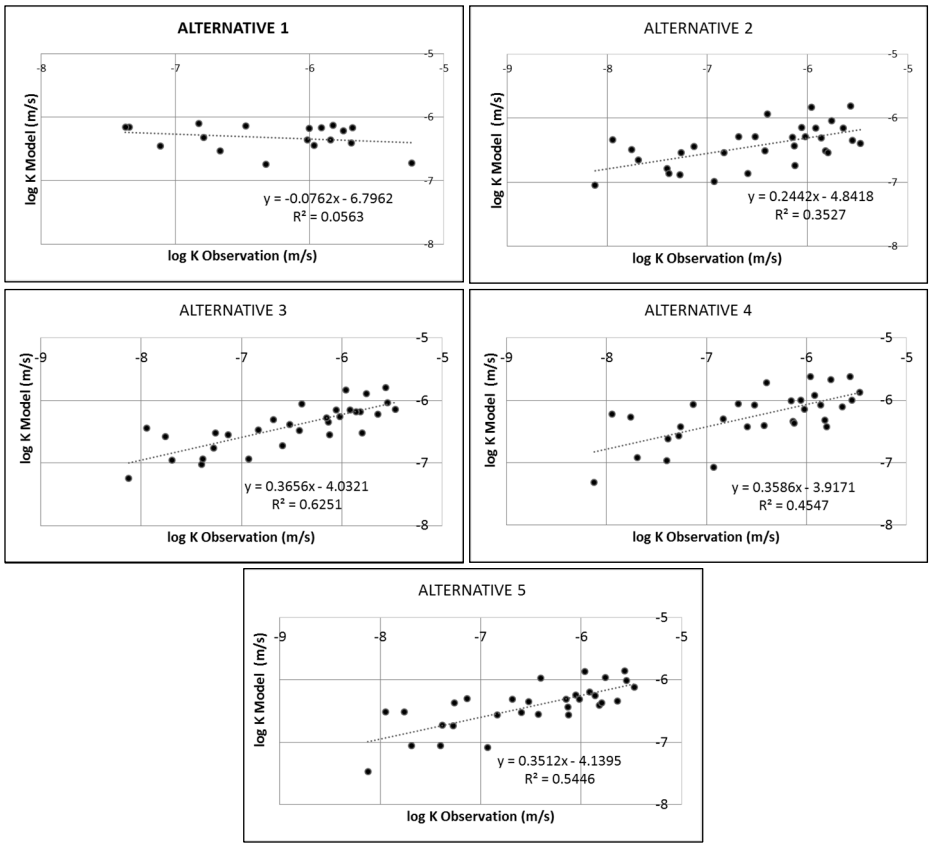

Figure 7 Comparison of validation of modeled K values using OK and observed K values.

5.3 Artificial Neural Network (ANN)

ANN is a soft computing method following the idea of basic biological neuron processing, which does not require determining a specific function expression. It only needs a connection between input and output variables with training and prediction analysis [9]. In this study, training and testing were carried out using a segmentation method that was developed by Mabruri, *et al.* [10]. This is a new method in stepwise training and testing, which was applied for unsampled points using ANN.

The best ANN architecture in this study was achieved using 9 nodes, 5 sequence data, and 2 hidden layers, as shown in Figure 8. The first hidden layer used a log-sigmoid (logsig) transfer function, while the second hidden layer used a

purely linear transfer function. Thus, every result was summed linearly. The Levenberg-Marquardt algorithm was used for training.

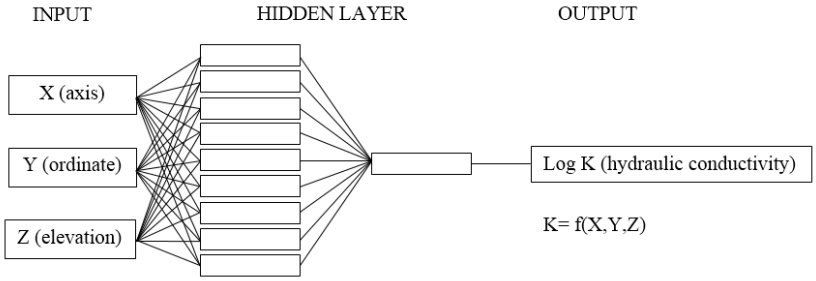

Figure 8 Architecture of ANN.

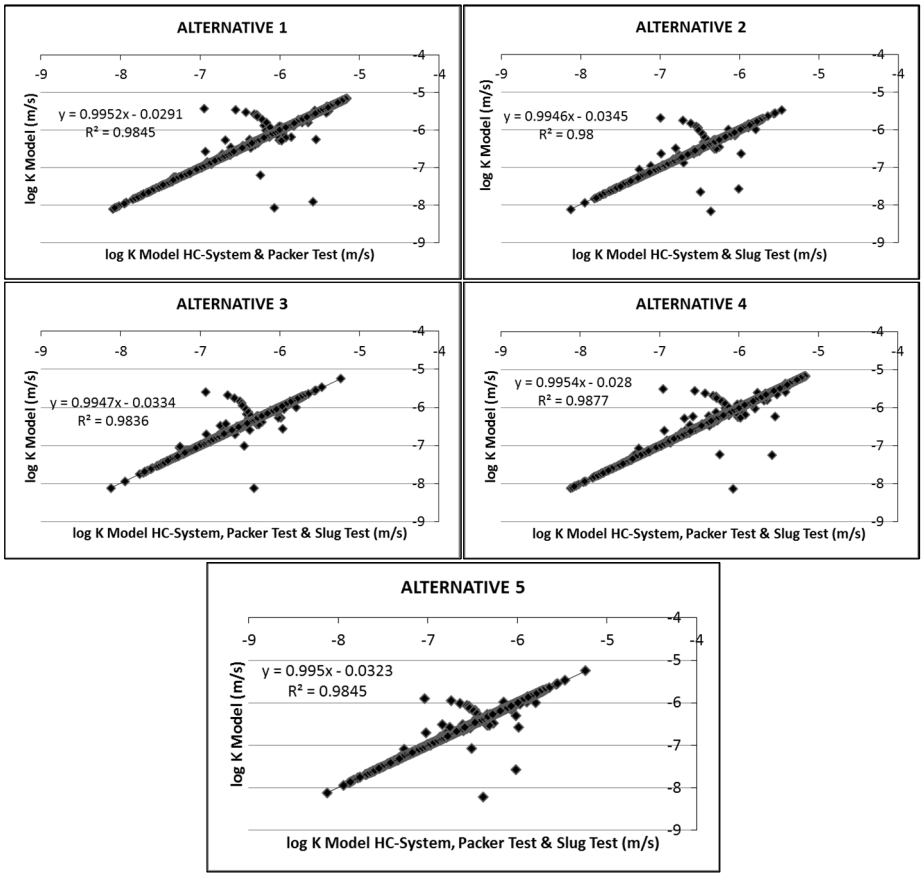

Figure 9 Comparison of validation of modeled K values using ANN and observed K values.

In this study, the original data were sorted based on depth (Z), and then a customized ANN was trained for the first 5 upper data to model log K distribution from surface depth to the 5th depth data. Furthermore, a new customized ANN was also trained for data numbers 2-6. This was applied continuously until the last step of the customized ANN had trained data numbers 4,846-4,850. Z (depth) segmented training was selected in every Z segment, because the data were distributed normally in the XY plane. A total of 4,845 network functions from the training process formulated by ANN were used to predict the hydraulic conductivity distribution. After training, prediction of K distribution was continuously made on the XY plane.

The best performance with MSE $<10^{-10}$ was used to control the quality of the training. Each trained segment was used to predict log K spatial distribution in its segment range, and every segment of spatial distribution data was combined to obtain the final model result. Verification and cross validation were then conducted following prediction according to ANN. This showed that the training was successful in estimating weighting and vice versa. Thus, all alternatives seemed to give a higher coefficient of determination (Figure 9).

6 Discussion

6.1 Statistics Approach

Statistical analysis based on the hydrogeological parameter study was required to determine the best alternative hydraulic conductivity model. The result of the statistical analysis of the observed and the modeled hydraulic conductivity distribution is listed in Table 4. Alternative 3 was considered to be the best alternative because of the following two reasons. Firstly, it relies on all

Table 4 Statistical summary of log hydraulic conductivity.

Alternative 3	Observation	HC model	ANN	OK
Amount of data	49	4.851	1.037.680	1.036.681
Minimum value (log K) m/s	-8.12	-7.72	-10.51	-8.12
First quartile (log K) m/s	-7.40	-7.21	-8.65	-7.53
Median (log K) m/s	-6.68	-6.71	-6.80	-6.94
Second quartile (log K) m/s	-5.96	-6.21	-4.94	-6.34
Maximum value (log K) m/s	-5.24	-5.70	-3.09	-5.75
Mean (log K) m/s	-6.43	-6.37	-6.60	-6.32
Standard deviation	0.73	0.33	0.87	0.25
Variance	0.53	0.11	0.76	0.06
Skewedness	-0.58	-0.63	-0.70	-0.59

observed information, from 49 points in total. Secondly, it resulted in the smallest difference between observed mean and modeled mean according to all

methods. With Alternative 3, ANN had the best K values, however these were not suitable when compared to the population of observation. The observed hydraulic conductivity values ranged between log -8.12 m/s and log -5.24 m/s. The ANN method gave a distribution with log K ranging from -10.51 m/s to log -3.09 m/s. Meanwhile, the OK method gave hydraulic conductivity values with log K ranging from -8.12 m/s to log -5.75 m/s. The ANN result yielded a slightly wider range of predicted values due to the absence of restrictions in the model construction. The OK model is strongly controlled by the semivariogram.

6.2 Best Alternative

HC-system was designed to estimate hydraulic conductivity values using in-situ rock properties [6]. According to the regression analysis of the alternatives, it can be concluded that the model shows good correlation between the HC index and hydraulic conductivity. Geological complexity may have an impact on water flow in fractured media in different ways, thus also influencing the

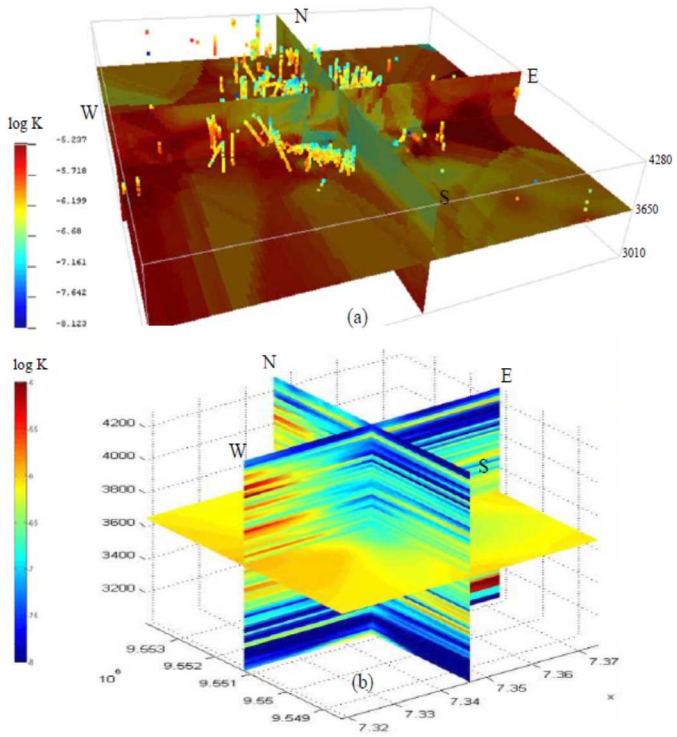

Figure 10 3D hydraulic conductivity models: (a) using OK method, (b) using ANN method.

complexity of the hydraulic conductivity estimation. The most significant or major component of HC-system in this case was RQD. It is suitable for the conceptual groundwater model of the Grasberg Mine, which is controlled by secondary aquifers and overburden primary aquifers. According to the statistical summary from the five alternatives, the third alternative using OK is considered to be the best model. The 3D models of hydraulic conductivity using OK and ANN are shown in Figure 10.

Figure 10(a) shows the hydraulic conductivity distribution resulted from the OK method with images of the circular area effect. The circle is formed by a semivariogram parameter that was previously set. Figure 10(b) shows the interpretation result of the hydraulic conductivity distribution using the ANN method, which is layer-shaped. This is due to the segmented interpolation in the horizontal plane resulted from the ANN method. The method can predict hydraulic conductivity at locations where values are not available by using the RQD and LPI variables. Predicted hydraulic conductivity at unsampled points should be clustered.

7 Conclusion

In this study numerical analysis using HC-system was employed to develop spatial distribution models of hydraulic conductivity based on hydrogeological, geotechnical and geological data. HC-system can be used to estimate K values in a zone where field test data are not available. However, geotechnical log data, i.e. RQD, LPI, GCD and DI, must be available. Reproducibility of hydraulic conductivity prediction with HC-system relies significantly on a large number of observational data. More data availability will provide a better correlation to the model. The 3D hydraulic conductivity model using OK was the best performing model out of five alternatives. It is expressed by equation $K = 2 \times 10^{-6} \times (HC)^{0.5571}$ with $R^2 = 0.716$. The log of hydraulic conductivity ranged from -8.12 m/s to -5.75 m/s. The ANN method also provided a fair interpretation. This is due to the segmented interpolation in the horizontal plane. Predicted hydraulic conductivity at unsampled points should be clustered and correlated to specific rock properties, such as RQD and LPI.

Acknowledgements

This research was supported by Dr. Irwan Iskandar, who is a researcher at Earth Resource Exploration Group ITB. The authors would like to thank the management of PT Freeport Indonesia for permission to publish this paper. The contributions made by Hafid Mabruri, Erlisa Yuwanita, Vellia Fatimah, and Dr. Agus Haris Widayat in improving the scripting and English writing of this paper are gratefully acknowledged.

References

[1] Singhal, B. & Gupta, R.P., *Applied Hydrogeology of Fractured Rocks*, 2nd Edition, Springer, New York, 408 pp., 2010.

[2] Zimmerman, R.W. & Bodvarsson, G.S., *Hydraulic Conductivity of Rock Fractures,* Transp Porous Media, **23**(1), pp. 1-30, 1996.

[3] Carlsson, A. & Olsson, T., *Hydraulic Properties of Swedish Crystalline Rocks-Hydraulic Conductivity and Its Relation to Depth*, Bulletin of the Geological Institute, University of Uppsala, pp. 71-84, 1977.

[4] Wei, Z.Q., Egger, P. & Descoeudres, F., *Permeability Predictions for Jointed Rock Masses*, International Journal of Rock Mechanics, Mineral Science and Geomechanics, **32**, pp. 251-261, 1995.

[5] Bellin, J., Mohr, P. & Rex, A., *Integrated Geotechnical Hydrogeological Field Programs in Open Pit Mining a Win-Win Situation?* In: Eberhard E, Stead D (eds.) Slope Stability 2011, Proceedings of the International Symposium on Slope Stability in Open Pit Mining and Civil Engineering, Vancouver, Canada, September 18-21, p. 10, 2011.

[6] Hsu, S., Lo, H., Chi, S. & Ku, C., *Rock Mass Hydraulic Conductivity Estimated By Two Empirical Models*. In: Dikinya O (ed.) Developments in hydraulic conductivity research. InTech, New York, pp. 134-158, 2011.

[7] Teles, V., Delay, F. & Marsily, G., *Comparison of Transport Simulations and Equivalent Dispersion Coefficients in Heterogeneous Media Generated by Different Numerical Methods: a Genesis Model and a Simple Geostatistical Sequential Gaussian Simulator*, Geological Society of America, Geosphere, **2**(5), pp. 275-286, 2006.

[8] Cahyadi, T.A., Notosiswoyo, S., Widodo, L.E., Iskandar, I. & Suyono, *Hydraulic Conductivity Distribution from Aquifer Test Result Constant Head Permeability in Sedimentary Rock*, Proceeding TPT Perhapi XXIII, pp. 352-360, 2014. (Text in Indonesian)

[9] Schaap, M.G. & Bouten, W., *Modeling Water Retention Curves of Sandy Soils Using Neural Networks*, Water Resources, **32**(10), pp. 3033-3040, 1996.

[10] Mabruri, H., Cahyadi, T.A., Widodo, L.E. & Iskandar, I., *Modeling of 3D Isotropic Distribution of Hydraulic Conductivity using Neural Network*, Proceeding ICAST, ITS and Kumamoto University, pp. 47-48, 2015.

[11] MacDonald, G., & Arnold, L., *Geological and Geochemical Zoning of the Grasberg Igneous Complex, Irian Jaya, Indonesia,* Journal of Geochemical Exploration, **50**, pp. 143-178, 1994.

[12] McDowell, F., *Pliocene Cu-Au Bearing Igneous Intrusions of the Gunung Bijih District, Irian Jaya, Indonesia, K-Ar Geochronology*, Journal of Geology, **104**, pp. 327-340, 1996.

[13] Suwardy, E. & Margotomo, W., *Geology and Hydrothermal Characteristics Zone Alteration, Mineralization Deposition In Contacts intrusion in Grasberg Copper-Gold Porphyry-Irian Jaya*, Proceeding IAGI XXVII, 1998. (Text in Indonesian)

[14] Hill, K., Kendrick, R., Crowhurst, P. & Gow, P., *Copper-Gold Mineralization in New Guinea: Tectonics, Lineaments, Thermochronology and Structure*, Australian Journal of Earth Sciences, Vol.49, pp. 737-752, 2002.

[15] Antoro, B., Margotomo, W., Perdana, A., Widijanto, E., Wiwoho. N., Ginting, A.P., Santosa, R.G.I., Pramuji, Silaen, H., Setyadi, H., Iribaram, F., Mundu, S., Garjito, W., Sumarwan, F., Rohmadi, A., Setiadi, T., Afwan, A., Asrizal., Pahala, A.R. & Prasetyo, N., *Geology and Geotechnic Grasberg Open Pit Mining, PTFI,* Aksara Buana, 2011. (Text in Indonesian)

[16] Silaen, H., Pramuji., Ginting, A., Widyanto, D. & Waromi, I., *Hydrogeological and Pore Water Pressure Characterization At South West Sector of Grasberg Open Pit, Papua*, Proceedings JCM Makassar The 36th HAGI and 40th IAGI Annual Convention and Exhibition, 2011.

[17] Iskandar, I., Wibowo, A., Casanova, B. & Notosiswoyo, S., *A 3D Model of Hydraulic Conductivity Distribution of Fractured Rocks Using Packer Test Result and Geotechnical Log*, International Symposium on Earth Science and Technology, University of Kyushu, Japan, 2014.

[18] Deere, D.U., Hendron, A.J., Patton, F. D. & Cording, E.J., *Design of Surface and Near Surface Construction In Rock*, Proceedings of 8th U.S. Symposium, Rock Mechanics, AIME, pp. 237-302, New York, 1967.

[19] Singhal, B.B.S. & Gupta, R.P., *Applied Hydrogeology of Fractured Rocks,* Kluwer Academic Publishers, The Netherlands, 400 p., 1999.

[20] Spitz, K., & Moreno, J., *A Practical Guide to Groundwater and Solute Transport Modeling*, John Wiley, New York, 480 p., 1996.

[21] Bear, J., *Dynamics of Fluids in Porous Media*, American Elsevier Publication Co., New York, 1972.

[22] Remy, N. & Boucher A., SGeMS v2.5b http://sgems.sourceforge.net/, (2 April 2014).